

Magnetic QCA Majority Voter Feasibility Analysis

Original

Magnetic QCA Majority Voter Feasibility Analysis / Vacca, Marco; Vighetti, D.; Mascarino, M.; Amaru', L. G.; Graziano, Mariagrazia; Zamboni, Maurizio. - STAMPA. - (2011), pp. 229-232. (Intervento presentato al convegno International Conference on Ph.D. Research in Microelectronics and Electronics (PRIME) tenutosi a Trento nel July 2011) [10.1109/PRIME.2011.5966275].

Availability:

This version is available at: 11583/2479782 since:

Publisher:

IEEE

Published

DOI:10.1109/PRIME.2011.5966275

Terms of use:

openAccess

This article is made available under terms and conditions as specified in the corresponding bibliographic description in the repository

Publisher copyright

(Article begins on next page)

Magnetic QCA Majority Voter Feasibility Analysis

M.Vacca, D.Vighetti, M.Mascarino, L.G.Amaru, M.Graziano and M.Zamboni
Electronics Department, Politecnico di Torino, Italy

Abstract—With the continuous scaling of CMOS transistors size, the interest on emerging technologies is rapidly arising. Among the “beyond CMOS” alternatives, Quantum dot Cellular Automata represent an innovative way to implement digital circuits. Particularly, the magnetic implementation (MQCA) favours the fabrication of circuits with a tiny power dissipation and with intrinsic memory capability.

Despite many works have already demonstrated the possibility to fabricate this kind of circuits, many efforts are still required to obtain a better comprehension of the design issues related to the basic logic blocks. In this contribution we deeply analyse the key logic gate of MQCA circuits, the Majority Voter (MV), taking into account its physical feasibility and its consequent expected performance. Detailed simulations of the MV are here reported, based on accurate finite-elements micromagnetic simulators; in order to demonstrate the range of operation of the device the distance among nanomagnets and their aspect ratio are used as key parameters. This range of operation represents the technological tolerance that the fabrication process must respect. We have also performed a timing analysis of the gate, demonstrating not only the absolute delay of the circuit, but also the delays obtained with different input configurations. Results show how the delay of the gate changes if the distances between neighbour magnets is varied, demonstrating that the choice of the distances must be carefully done in order to balance the physical feasibility and the gate delay.

I. INTRODUCTION

Quantum dot Cellular Automata are a new technology, candidate to substitute CMOS transistors according to International Technology Roadmap of Semiconductors [1]. The logic value is represented using cells with bistable charge configuration, that have only two stable states [2], i.e. logic values ‘0’ and ‘1’. Magnetic QCA (also called NML - nanomagnetic logic) [3][4] represent one of the most interesting implementation of this principle. Rectangular shaped nanomagnets, small enough to be approximated as single domain magnetic devices, are used as base cells. Due to shape anisotropy nanomagnets have only two stable magnetizations, aligned to the long side of the magnet. Despite the limited speed that these circuits can reach (about 100MHz), they can be interesting for all those applications where speed is not a key point, but where power consumption is crucial (e.g. smart sensors, biological sensors,...) [5]. Magnetic logic has indeed an expected power absorption hundred of times smaller than CMOS circuits. Moreover it shows an intrinsic memory capability, because the base device is a magnet which can maintain information stored without the need of power supply.

It has been demonstrated [6] that for QCA circuits an adiabatic switching is required. An external field drives the cells in an intermediate unstable state, with the aim of facilitating the switching between stable states. This signal is called “clock”

and, in this case, is a magnetic field, parallel to the short side of the magnets [6]. It is generated by the current flowing through a wire buried under the nanomagnets plane. A multiphase clock system is necessary [3] to assure an errorless information propagation, as shown in figure 1. As proposed in our previous works [7][8], three clock signals, with a phase difference of 120 degrees, are applied to different areas of the circuit. These areas include a limited number of nanomagnets and are generally called “clock zones”. The operation of this clocking system is shown in figure 1.

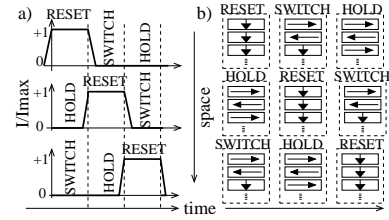


Fig. 1. A) Clock signals waveform. A 120 degree phase difference occurs between every couple of phases. B) Signal propagation: At every time step magnets in one clock zone are in the SWITCH phase, those in the previous clock zone are in the HOLD phase and act like an input, those in the next clock zone are in the RESET phase and have no influence on the others.

At every time step each clock zone can be in one of three different states: HOLD, SWITCH, RESET. When the magnetic field is applied, nanomagnets are in the RESET phase, their magnetization is directed along their short axis and they have no influence on the neighbour magnets. When the field is removed (it passes from a maximum value to zero), nanomagnets are in the SWITCH phase. They start to realign following the neighbour nanomagnets that are still in the HOLD state. When there is no field applied, at the end of the switch phase, nanomagnets are in the HOLD phase, they have a stable magnetization and influence neighbour magnets. In this way information is correctly propagated through the circuit. At the following time step this situation is repeated, but the switching zone is the next one, as shown in figure 1.

Many works analyzed the behavior of nanomagnets [3][4] with the attention on the single magnet and its optimal shape. In this contribution we focus on the most relevant logic block, the Majority Voter (MV), on its physical feasibility in terms of distance, size, and aspect ratio of the magnets, using an accurate finite elements nanomagnetic simulator [9]. As an absolute novelty in the literature we found the operating zone allowed for the MV to work correctly. Moreover, dynamic conditions were characterized, obtaining switching times for the whole MV as a function of several parameters, considerably advancing the scientific knowledge about MQCA.

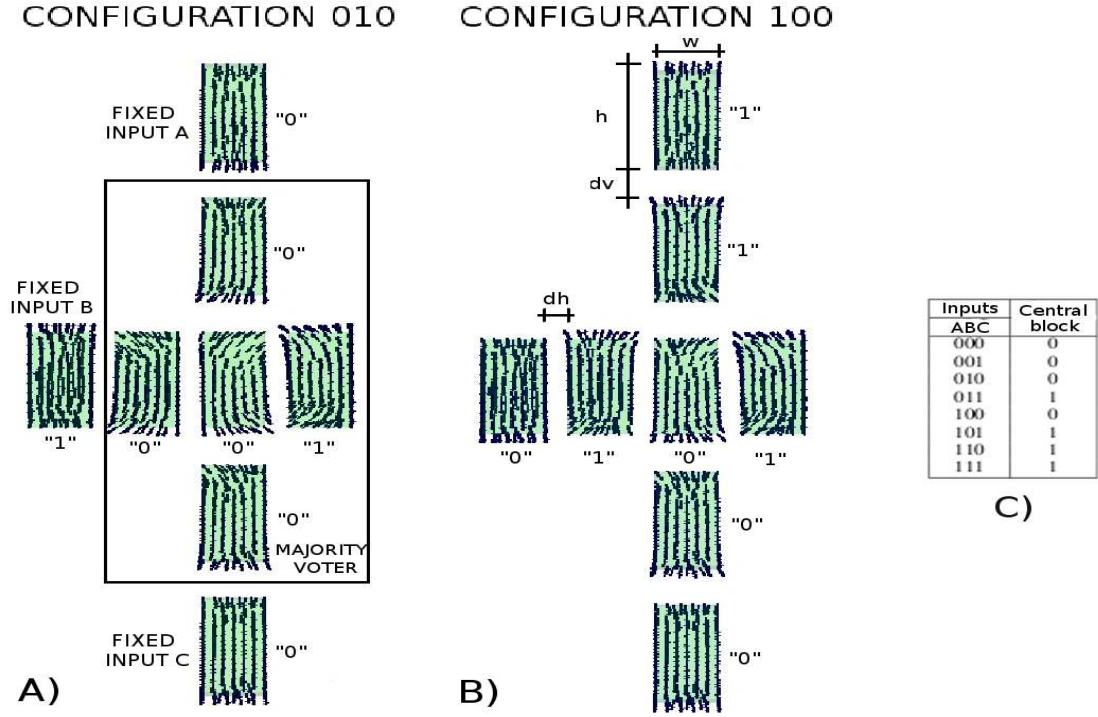


Fig. 2. Majority voter simulations. A) and B) represent the MV structure in two particular conditions at the end of the simulation based on NMAG, i.e. 010 and 100 respectively. C) gives the MV truth table.

II. MAJORITY VOTER CHARACTERIZATION

From the experimental point of view the major limitation to nanomagnets fabrication is the small distance between neighbour magnets. The gap between two magnets requires highly precise machines (Electron Beam Lithography, Focused Ion Beam Lithography). Moreover, the need for a so small gap has a strong impact on the quality of the patterned nanomagnets geometry. This is a strict limitation and, compared to the necessity of implementing nanometer scale elements, it has a strong impact on the experimental feasibility of this kind of circuits. For these reasons we have performed many simulations, using NMAG [9], a finite-difference open-source nanomagnetic simulator, changing parameters that can influence the experimental processes [11][10]. This work focuses on the Majority Voter (MV) which is the base logic block of this technology.

The basic structure of the MV is shown in figure 2. It is composed by 5 elements (bounded with a box in figure 2.A), i.e. 4 elements enclose a central element which executes the logic operation. The elements on the left and the upper and lower ones act like inputs, while the element on the right in the box is the output block. Three more blocks are present in the figure 2.A (external to the bounding box): these are magnets holding a fixed magnetization used to force the inputs of the MV in the desired state. Figures 2.A, and 2.B show the final configuration of the MV simulation with two among the eight possible input configurations (010 and 100 for A, B and C respectively). The logic '1' corresponds to the arrows pointed

up while the logic '0' corresponds to the arrows pointed down. The magnets alignment corresponds to the MV truth table (fig. 2.C)) where inputs and MV central block expected logic values are reported.

After verifying the MV correctness in all the combinations, we focused on its design parameters. The design space has been explored through several simulations, changing the horizontal and vertical distances (respectively dh and dv in figure 2.B) between nanomagnets and their aspect ratio (h/w in figure 2.B, where $h = 200nm$ and $w = 100nm$). We obtained from the simulations an operative range for the MV. Figure 3.A shows, for every input configuration, the combinations of horizontal and vertical distances assuring the expected output, when nanomagnets have a 2:1 aspect ratio. It is clear in all the cases that an increment of the horizontal distance requires an increase of the vertical distance to obtain a working configuration. Another interesting point is that every input configuration has a different working area, demonstrating that some configurations are more easy than others. In particular the 001 configuration is the most troublesome, while the 111 configuration has the biggest working range. If all these "maps" are merged together, we obtain the more constraining working area of the MV (figure 3.B left). These simulations were repeated changing the aspect ratio of the nanomagnets. Figure 3.B center and left show the working area of the MV using nanomagnets with an aspect ratio of 2.5:1 and 3:1, respectively. It is worth noticing that an aspect ratio increment reduces the effective solutions space, as particularly evident from the 3:1 aspect ratio condition. To summarize,

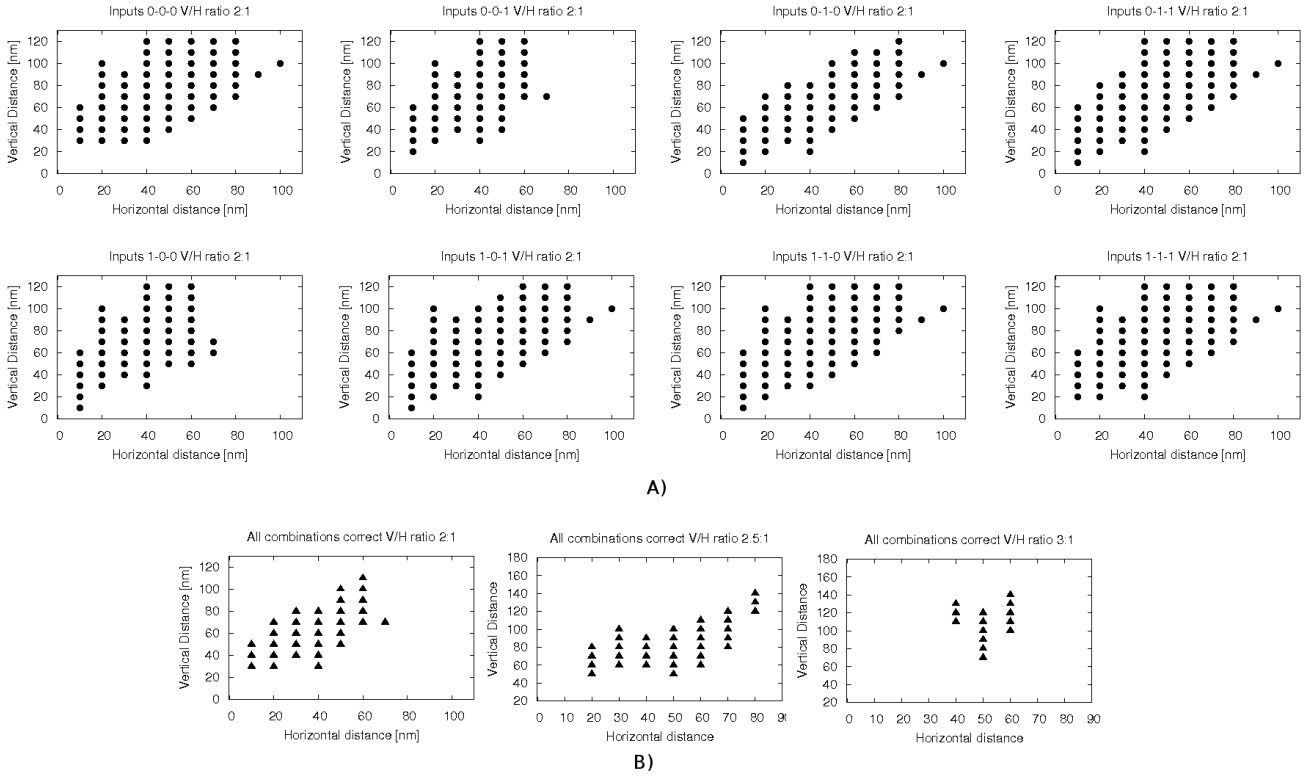


Fig. 3. Geometrical operative ranges for the Majority Voter. Points represent a vertical and horizontal gap between magnets which assure the correct MV behavior. A) Operative ranges for each MV input combination, where magnets have an aspect ratio of 2:1. B) Operative ranges considering all the combinations: left, center and right maps are for 2:1, 2.5:1 and 3:1 aspect ratio respectively.

the MV works also changing the relative distances between magnets, and this is promising as it means that technological tolerance does not prejudice the operations of magnetic QCA circuits. On the one hand, this technology works well with scaling down. On the other hand, even with distances of 60nm (horizontal) and 100nm (vertical), the MV is still working, and this is a very good result because these gaps are more feasible from the technological point of view, at least with the available technology. A gap of 100nm can be obtained using low-end electron beam lithography with a relative small acceleration voltage of 30kV, but, it can be obtained also with high-end optical lithography, which is a good promise for the commercial realization of this technology. Finally, the better aspect ratio is the 2:1, which grants the biggest working zone. This can be easily explained because, increasing the aspect ratio also increases the energy for the magnets switching.

III. TIMING ANALYSIS

The nanomagnets switching time was also derived from previous simulations. Figure 4 shows how the magnetization of the central element of the majority voter, which holds the logic function, changes in time. The different lines are related to simulations where vertical distances vary from 30nm to 80nm, while horizontal distance is fixed at 20nm. The two numbers represent the horizontal distance dh and the vertical one dv expressed in nanometers, respectively (for example M_20_40 means $dh = 20nm$ and $dv = 40nm$). Figure 4.A

shows a working case, i.e. the magnetization moves from 0 to a negative value, with inputs configuration 100 and an aspect ratio of 2:1. Figure 4.B shows the magnetization for the same choice of distances in case of 010 input configuration (aspect ratio 2:1). When the vertical distance is 80nm the magnetization, though initially decreasing, moves toward a wrong positive value. In the 70nm case the final result is correct, but the switching time is notably increased with respect to the other cases. In figure 4.C a table reports the switching time calculated as the delay from the instant in which the magnetization begins to move from the reset state, to the instant in which the magnetization reaches the 50% of the swing. It is reported here for all the input combinations in case of aspect ratio 2:1, horizontal distance 20nm and vertical distance 30nm, 50nm and 70nm.

It is worth noticing that the switching time depends on the input configuration and on the vertical distance of magnets. However this influences differently the switching time, depending on the input configuration. For example, in the 011 configuration, with the increase of the vertical distance, the switching time remains constant; but in the 010 configuration the vertical distance increment causes a proportional increase of switching time. The absolute switching time value is between 90ps and 260ps, which is the expected time evolution for this type of magnetic structures.

To obtain a more complete analysis of the majority voter delay, we repeated the above simulations according to the map

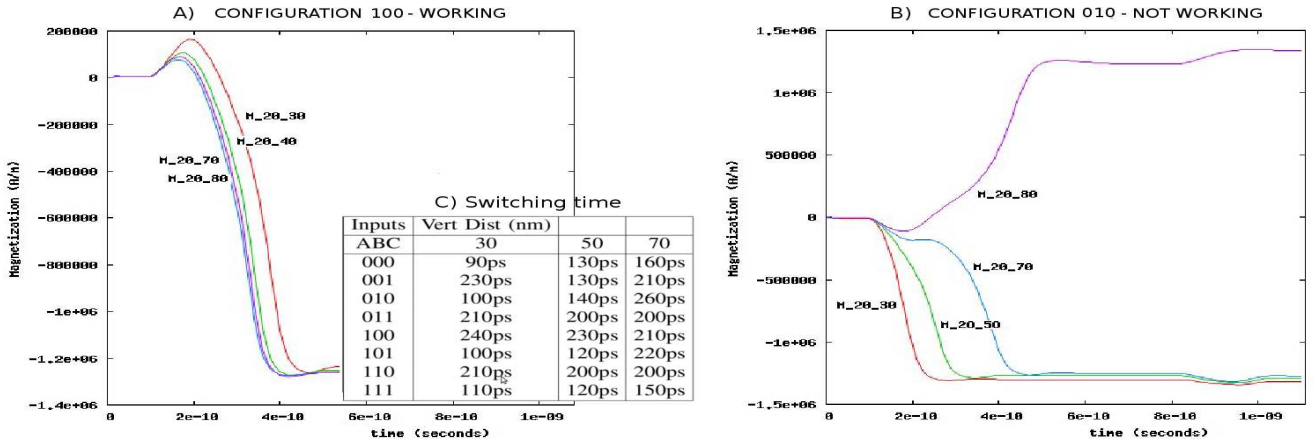


Fig. 4. Transient magnetization of the central MV's nanomagnet and switching times for two input configurations: 100 (A) and 010 (B). Curves are related to different vertical distances (from 30nm to 80nm), while the horizontal one is fixed (20nm). Combination 010 shows a wrong magnetization in the 80nm case. Table (C) shows 50% switching time for all the combinations.

of figure 3.B. Our focus was on the aspect ratio 2:1 which shows the best results. For all the points of the map, which represents the working area of the gate, we evaluated the switching time for all the MV input combinations. Results are summarized in figure 5. For every value of horizontal distance the minimum and maximum delay times obtained among all the eight combinations and the possible vertical distances are shown. From figure 5 can be clearly the influence of the distance on the gate delay can be clearly figured out. Increasing the distance causes a switching time rising. This delay increment can be considered, in first approximation, linear. These results demonstrate how the choice of the distance must be a careful one, as it requires a balance between technological issues and speed requirements.

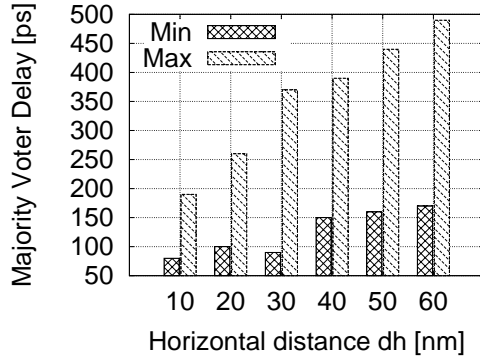


Fig. 5. MV timing characterization. For each horizontal distance the minimum and the maximum delay is reported.

IV. CONCLUSION

We accurately simulated in several conditions the magnetic QCA basic block, the Majority Voter, obtaining four main contributions. First, we demonstrated that this gate can operate even taking into account the tolerance of the productive process. Second, we found the space of design solutions in terms

of magnets distances: if the distance between neighbour nanomagnets is varied we still obtain a working gate, reducing thus the fabrication process constraints. Third, we demonstrated that nanomagnets of aspect ratio of 2:1 grant a wider solution space. Finally, we have analysed the MV switching time, defining its dependency from input configurations and relative distances between elements. If distances between nanomagnets are increased the gate switching time is also raised, therefore distances must be changed carefully to balance technological feasibility with circuits performance. We are currently working on an experimental demonstration of these results: an example of a FIB fabricated QCA wire is in figure 6.

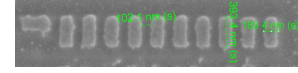


Fig. 6. Preliminary experiments on a QCA wire. Acknowledgements go to INRIM Institute and Compagnia di San Paolo for Nanofacility Piemonte.

REFERENCES

- [1] Semiconductor Industry Association, "International Technology Roadmap of Semiconductors", <http://public.itrs.net>, 2008.
- [2] C. S. Lent, P. D. Tougaw, W. Porod and G. H. Bernstein "Quantum cellular automata", *Nanotechnology*, Vol. 4, 49, 1993
- [3] A. Imre et al. "Investigation of shape-dependent switching of coupled nanomagnets", *Superlattices and Microstructures*, 34, 513-518, 2003.
- [4] A. Orlov et al. "Magnetic Quantum-Dot Cellular Automata: Recent Developments and Prospects", *ASP J. of Nanoelectronics and Optoelect.*, Vol3, N. 1, 2008.
- [5] G. Csaba et al. "Simulation of Power Gain and Dissipation in Field-Coupled Nanomagnets", *J. of Computational Electronics*, Springer, Vol. 4, 2005.
- [6] M.T. Alam et al. "Clock Scheme for Nanomagnet QCA", *Proc. of IEEE Int. Conf on Nanotechnology*, 2007.
- [7] M. Vacca "Magnetic QCA Nanoarchitectures", *Master Thesis*, Politecnico di Torino, November 2008.
- [8] M. Graziano et al. "A Technology Aware Magnetic QCA NCL-HDL Architecture", *Proc. IEEE Conf. on Nanotechnology*, Genova, July 2009.
- [9] <http://nmag.soton.ac.uk/nmag/>
- [10] M. Mascarino "Analysis and simulation of Circuits Based Magnetic QCA", *Master Thesis*, Politecnico di Torino, November 2009.
- [11] D. Vighetti "Nanomagnetic characterization of Magnetic QCA circuits", *Master Thesis*, Politecnico di Torino, July 2011 (to be completed).